COMPARISON OF THE TESLA, NLC AND CLIC BEAM-COLLIMATION SYSTEM PERFORMANCE*

A. Drozhdin[4], G. Blair[6], L. Keller[5], W. Kozanecki[2], T. Markiewicz[5], T. Maruyama[5], N. Mokhov[4], O. Napoly[2], T. Raubenheimer[5], D. Schulte[3], A. Seryi[5], P. Tenenbaum[5], N. Walker[1], M. Woodley[5], F. Zimmermann[3]. [1]DESY, Hamburg, Germany; [2]DSM/DAPNIA, CEA-Saclay, France; [3]CERN, Switzerland; [4]FNAL, Batavia, USA; [5]SLAC, Stanford, USA; [6]Royal Holloway College, UK

Abstract

This report describes studies performed in the framework of the Collimation Task Force organized to support the work of the second International Linear Collider Technical Review Committee. The post-linac beam-collimation systems in the TESLA, JLC/NLC and CLIC linear-collider designs are compared using the same computer code under the same assumptions. Their performance is quantified in terms of beam-halo and synchrotron-radiation collimation efficiency. The performance of the current designs varies across projects, and does not always meet the original design goals. But these comparisons suggest that achieving the required performance in a future linear collider is feasible.

INTRODUCTION

We present a summary of comparisons of the collimation-system performance for the three main candidate linear-collider designs: JLC/NLC, CLIC and TESLA. The essence of these results is included in Ref. [1] and more details can be found in Ref. [2].

For the next generation e^+e^- linear colliders (see [1] and Table 1), small fractional beam losses along the transport line, or the presence of particles far from the beam core in the IP region, may strongly affect the background conditions in the detector, as well as cause irradiation and heating of collider components.

Table 1: LC parameters for 500 GeV c.m.energy.

parameter	TESLA	NLC	CLIC
Bunch population, $E+10$	2	0.75	0.4
Number of bunches per train	2820	192	154
Separation between bunches, ns	337	1.4	0.67
Repetition frequency, Hz	5	120	200
Average current (each beam), μa	45.1	27.6	19.7
Beam power (each beam), MW	11.3	6.9	4.9
Normalized emitt. x,y, mm·mrad	10, 0.03	3.6, 0.04	2.0, 0.01
Beta function at IP, x,y, mm	15.2, 0.41	8, 0.11	10, 0.05
Beam size at IP, x,y, (σ), nm	553, 5	243, 3	202, 1.5

All machine designs need to remove this halo to a certain "collimation depth", which is generally set by the synchrotron-radiation fan generated by the halo particles in the last few magnets close to the IP: by definition, all particles within the collimation depth generate photons that should pass cleanly through the IR. Halo particles outside this collimation depth are removed by physically intercepting them with "collimators", which are formed by a thick absorber of many radiation lengths placed in the optical shadow of a thin spoiler, the thickness of which is generally less than one radiation length.

Analytic estimates predict halo of the order of 10^{-6} of the LC beam current. However, given the SLC experience, designers of collimation systems have taken the conservative approach to build a collimation system that would be able to intercept a fractional halo of 10^{-3} of the beam – the number we assumed for the present study.
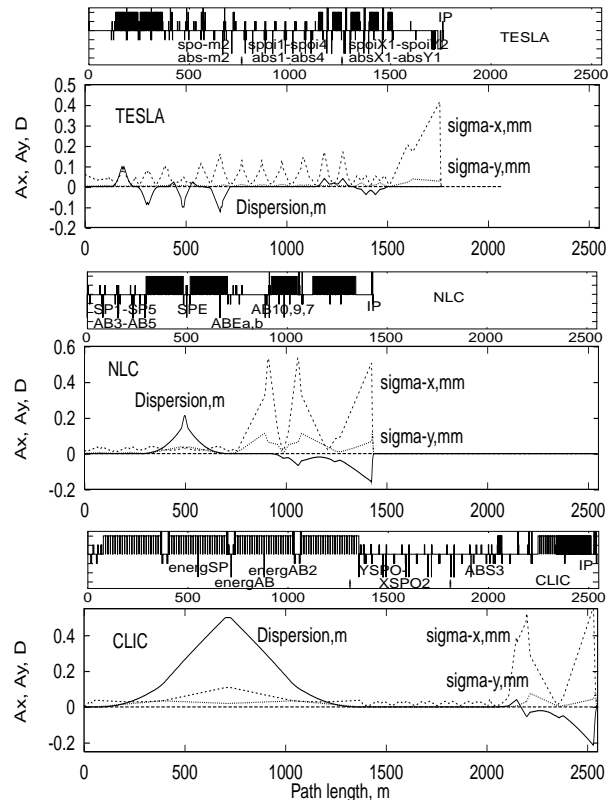

Figure 1: Collimator locations in TESLA, NLC and CLIC.

The comparative studies were carried out using the program STRUCT [3]. This package performs particle tracking, taking into account aperture restrictions, interaction of primary beam particles with collimators, beam losses, synchrotron radiation and transport of the photons along the beamline.

COLLIMATION IN LINEAR COLLIDERS

All designs have a dedicated primary collimation system (betatron and off-energy) located upstream of the final focus system (FFS). Additional secondary or "clean-up" collimators are located in the FFS. The maximum number of halo particles that may be intercepted in this secondary system is limited by the muon flux the detector can tolerate. The primary system — which intercepts most of the halo – should have high enough an "efficiency" to reduce the

losses in the secondary system to acceptable levels. At the same time, the combination of primary and secondary collimation must bring the halo population outside the collimation depth in the final doublets within tolerance.

Collimation of the beam requires putting material close to a beam with a high energy density, which in turn creates a risk that a missteered beam might destroy the collimator. In practice, in order to limit the betatron functions in the collimation region, the design relies on thin (0.5-1 radiation length) spoilers which scrape the halo with minimal heating and enlarge the spot size of a missteered beam via multiple Coulomb scattering and energy loss. The enlarged beam is then absorbed in thick (30 radiation lengths) copper absorbers. Absorbers in the primary collimation section should lie in the shadow of their spoiler partner to reduce the probability of being hit directly by a missteered beam.

Table 2 lists the physical properties of the spoilers and absorbers for the three machines. Fig. 1 shows collimator locations, horizontal dispersion and beam sizes in the BDS.

Table 2: Parameters and achieved performance of the post-linac primary collimation systems. $\sigma_{x,y}$ are the beam sizes at the primary spoiler (including the dispersive contribution); $\sigma_{x,y}^{\beta}$ refer to the betatron contributions alone. The spoiler settings are tighter than the effective collimation depth at the FD due to dispersive and higher-order effects.

		TESLA	JLC-X/NLC	CLIC
Nominal collimation depth (at spoiler)	# $\sigma_{x,y}^{\beta}$	12, 74	10, 31	9, 65
Energy collimator	x gap, mm	3.0	6.4	3.2
	$\sigma_{x,y}, \mu m$	154, 4.5	534, 29	814, 38
Betatron collimator Final-doublet phase	x, y gaps, mm	3.0, 1.0	0.6, 0.4	0.68, 0.4
	$\sigma_{x,y}, \mu m$	129, 7	28, 6.5	38, 3
IP phase	x, y gaps, mm	3.0, 1.0	0.6, 0.5	0.6, 0.4
	$\sigma_{x,y}, \mu m$	128, 7	16, 0.8	22, 3
Effective collimation depth (at FD)	# $\sigma_{x,y}^{\beta}$	13, 80	15, 31	11, 100
Spoiler material		Ti	Cu + Be	
Spoiler length	mm (rad.length)	35 (1)	117 ($0.5_{Cu} + 0.3_{Be}$)	
Absorber length	mm (rad.length)	500 (35)	429 (30)	
Achieved primary-collim. efficiency		0.01	$< 1 \cdot 10^{-5}$	$< 3 \cdot 10^{-4}$
Losses in secondary collimation section	part./bunch	$2.4 \cdot 10^5$	50	1000

RESULTS

Methodology

The effectiveness of the collimation system can be quantified in terms of: a) the fraction of initial halo particles that survive (or are rescattered out of) the primary collimation system and hit secondary collimators or other aperture limitations closer to the IP (this is relevant when estimating muon backgrounds); b) the number of halo particles that lie outside the collimation depth when they reach the final doublet (this is relevant when estimating synchrotron-radiation backgrounds).

For simulations of the effectiveness of the three collimation systems and of background conditions at the IP, the beam halo was represented by a large number of rays (typically 5×10^5) distributed in phase space with $1/r$ amplitude distributions and with a Gaussian momentum distribution of $\sigma(dP/P) = 1\%$.
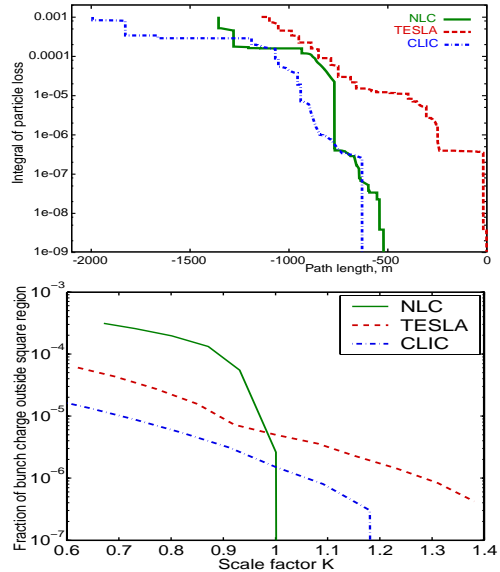

Figure 2: Collimation-system performance assuming an incident fractional halo of 10^{-3}. Top: fractional loss of charged-halo particles, integrating back, starting at the IP. The horizontal scale shows the distance from the IP. Bottom: number of charged-halo particles per bunch, normalized to the nominal bunch charge, in a rectangular $x-y$ window at the entrance to the final doublet, as a function of the collimation depth. The scale factor K defines the window dimension: for $K=1$, the window size corresponds to the effective collimation depth listed in Table 2.

Primary-collimation Efficiency

Figure 2 (top) displays, for each machine, the cumulative particle loss, starting at the IP and integrating back to the entrance of the collimation system.

- The NLC design achieves a primary-collimation efficiency significantly better than 10^{-5}, resulting in less than 10^4 particles per train being lost in the secondary system.

- In TESLA, with the primary collimation as currently designed, the loss rate in the secondary system amounts to about 1% of the initial halo population. Because the TESLA bunch spacing is longer than the entire bunch train for the warm machines, TESLA generally quotes background rates per bunch crossing. However the subdetector most sensitive to muon background, the time projection chamber (TPC), integrates over 150 bunches, so that for the same assumed incident halo fraction of 10^{-3}, the effective halo population becomes similar to that of NLC and the effective loss in the secondary collimation system amounts to $3 \cdot 10^7$ particles per sensitivity window.

- The CLIC collimation system achieves a primary-collimation efficiency of about 3×10^{-4}.

Halo Photons

The collimation-system performance achieved at the entrance to the final doublet, and the resulting level of halo-induced SR backgrounds, are summarized in Tables 3 and 4. They can be characterized as follows.

In NLC, the edge of the collimation depth is sharply defined (Fig. 2 bottom); but for no halo photons to hit

Table 3: Synchrotron radiation from the beam halo near the IP. The number of bunches per 'effective' train reflects the sensitivity window of the time projection chamber (TPC).

	TESLA	JLC-X/NLC	CLIC
# bunches/(effective train)	150	192	154
Losses on SR mask upstream of FD			
Mean photon energy (MeV)	0.474	0.031	0.032
# photons/bunch	$1.4 \cdot 10^6$	$4.5 \cdot 10^5$	$8.5 \cdot 10^3$
# photons/eff. train	$2.1 \cdot 10^8$	$8.7 \cdot 10^7$	$1.3 \cdot 10^6$
Total photon energy (GeV) /bunch (/eff. train)	670 (100000)	14 (2700)	0.28 (43)
Charged halo (part./bunch)	7440	(none)	(none)
Losses on upstream detector mask			
Radius, mm	12	10 (QD0)	13
Photon losses, mW	0.03	0	$1.8 \cdot 10^{-6}$
Photon losses, GeV/bunch	13	0	$3.8 \cdot 10^{-4}$
Losses on vertex detector			
Radius, mm	-	10	13
Photon losses, mW	-	$< 10^{-7}$	$1.6 \cdot 10^{-3}$
Photon losses, GeV/bunch	-	$< 2.7 \cdot 10^{-5}$	0.33
Losses on downstream detector mask			
Radius, mm	12	13 (lum. monitor)	13
Photon losses, mW (GeV/bunch)	0.36 (158)	0	0.011 (2.2)
Losses on SR mask downstream of outgoing-side FD			
Mean photon energy (MeV)	10.1	-	-
# photons/bunch	$1.2 \cdot 10^7$	-	-
# photons/eff. train	$1.8 \cdot 10^9$	-	-
Total photon energy (GeV) /bunch	$1.2 \cdot 10^5$	-	-
/eff. train	$1.8 \cdot 10^7$	-	-
Charged halo (part./bunch)	246	-	-

the beam pipe near the IP, rather tight collimator settings (± 0.2–0.3 mm) are needed[1]. The halo photon flux hitting the FD SR mask on the incoming-side (Table 3) is low enough; in addition, these photons are rather soft ($\langle E_\gamma \rangle \sim$ 31 KeV). The halo hitting the detector masks and the vertex detector is negligible. Photon losses in the outgoing beam line were not calculated for NLC or CLIC because it was assumed that the crossing-angle geometry provides enough flexibility for an ample stay-clear on the spent-beam side.

In TESLA, the boundary of the collimated halo is barely visible. Charged-halo losses on the SR mask amount to about 7400 particles/bunch on the upstream side, and about 250 particles/bunch on the downstream mask. Simulations also indicate that some SR photons from the halo ($> 10^5$ photons/bunch) hit the detector mask located 3 m downstream of IP; their total energy (158 GeV/bunch) is however small compared to that of beam-beam induced pairs. More importantly, one observes a sizeable outgoing photon halo ($\sim 1.2 \times 10^5$ GeV/bunch, corresponding to about 1.2×10^7 photons) hitting the downstream SR mask 18 m from the IP: the total energy of the halo photons intercepted by this mask is about half of that deposited by outgoing SR photons from the beam core hitting the same mask (Table 4). Both the mean energy (Table 3) and the number of halo photons per pulse is an order of magnitude larger in TESLA than in NLC, because of significantly stronger bending fields. This remark also applies to SR photons radiated by the core of the incoming $e^\pm$ beam.

The halo in CLIC-500 appears reasonably well-behaved, and the number of photons hitting the SR and IR masks is

of no concern. This promising performance was however obtained with rather tight collimator settings. Detailed simulations of the 500 GeV CLIC system are only beginning, and its collimator configuration is still in flux.

Synchrotron Radiation from the Beam Core

A sizeable flux of SR photons produced by the beam core (primarily in the last dipole) hits the SR masks on either side of the IP (Table 4). In NLC, when integrated over the entire bunch train, the flux of SR photons from the core reaches a level that may deserve attention. In TESLA, about 10^{10} core photons/bunch hit the SR mask upstream of the IP, depositing 10^9 GeV/effective bunch train. While it is plausible that the effectiveness of the TESLA collimation system may be further improved, these results underscore the urgent need for more detailed studies. In CLIC, the flux of intercepted core SR photons is slightly lower than in NLC, presumably due to the fact that the CLIC IR has been optimized for 3 TeV c.m. energy.

Table 4: SR from the beam core hitting IR masks.

	TESLA	NLC	CLIC-500
Losses upstream of FD			
Mean photon energy (MeV)	0.450	0.032	0.034
# photons/bunch	$1.4 \cdot 10^{10}$	$0.9 \cdot 10^9$	$5.9 \cdot 10^8$
# photons/eff. train	$2.1 \cdot 10^{12}$	$1.7 \cdot 10^{11}$	$9.1 \cdot 10^{10}$
Total photon energy (GeV) /bunch	$6.2 \cdot 10^6$	$3.0 \cdot 10^4$	$2.0 \cdot 10^4$
/eff. train	$9.3 \cdot 10^8$	$5.8 \cdot 10^6$	$3.1 \cdot 10^6$
Losses downstream of outgoing FD			
Mean photon energy (MeV)	0.467	-	-
# photons/bunch	$4.7 \cdot 10^8$	-	-
# photons/eff. train	$7.1 \cdot 10^{10}$	-	-
Total photon energy (GeV) /bunch	$2.2 \cdot 10^5$	-	-
/eff. train	$3.3 \cdot 10^7$	-	-

Further plans include continuing studies of muon backgrounds, evaluation of performance in a non-ideally tuned BDS with both static and dynamic errors, etc. [6].

SUMMARY

Comparative studies of the performance of the post-linac beam-collimation systems in the TESLA, NLC and CLIC designs have shown that the performance of the systems as currently designed is not uniform across projects, and that it does not always meet all the design goals. As of this writing, the CLIC and NLC collimation schemes appear the most promising. Improvements of the TESLA collimation system are expected to result from the ongoing overhaul of their BDS design [5]. Overall, the very existence of an acceptable solution suggests that achieving the required performance in future linear colliders is feasible.

REFERENCES

[1] Second ILC-TRC Report, SLAC-R-606, 2003.

[2] A. Drozhdin, *et. al.*, FERMILAB-TM-2200, 2003.

[3] A. Drozhdin, *et. al.*, 'STRUCT Program User's Reference Manual', http://www-ap.fnal.gov/~drozhdin/

[4] A. Drozhdin, *et. al.*, LCC-118, SLAC, to be published.

[5] J. Payet, O. Napoly, N. Walker, these proceedings.

[6] Collimation Task Force Workshop, SLAC, Dec. 2002, http://www-project.slac.stanford.edu/lc/wkshp/colltf2002/

---

[1]Here we present only the more pessimistic case, i.e. without tail folding octupoles, included in NLC BDS, which allow widening the spoiler gaps by a factor of 3 to 4. NLC collimation performance with these octupoles is discussed in Ref. [4].